*CLEAN – Soil, Air, Water*

WILEY-VCH

CLEAN Soil Air Water

RESEARCH ARTICLE

# Design Matters: Investigating Solute Leaching Dynamics With Multicolumn Experiments and Dual-Porosity Inverse Modeling

Clémence Pirlot | Aurore Degré

ULiège, Gembloux Agro-Bio Tech, TERRA Teaching and Research Centre, Gembloux, Belgium

**Correspondence:** Clémence Pirlot (clemence.pirlot@uliege.be)

**Received:** 27 May 2025 | **Revised:** 4 February 2026 | **Accepted:** 25 February 2026

**Keywords:** column diameter | column height | dispersivity | preferential flow | sampling method | soil structure

## ABSTRACT

Soil column experiments are widely used to study contaminant leaching, but variations in methodological designs can strongly affect transport results and risk assessments. This study quantitatively evaluates the influence of four key factors: sampling method, soil structure, column dimensions, and the presence of stratified layers. Twenty-one columns were built using silty agricultural soil, including both disturbed and intact cores, with diameters of 8.4 and 24 cm and heights of 20 and 35 cm. Columns were sampled either manually or with a mechanical corer. Tracer leaching experiments were conducted, and dual-porosity (DP) inverse modeling with Hydrus 1-D was used to determine water and solute mobility parameters. The results demonstrate that soil structure, column dimensions, and sampling techniques strongly affect water and solute transport dynamics. Soil structure has a critical influence on solute transport dynamics. Disturbed columns tend to underestimate the rapid transport of contaminants and overestimate their retention, providing an unreliable representation of groundwater contamination risk. Column diameter had limited effect in disturbed soils, but larger columns exhibited increased mobile zone fractions. Column height significantly influenced the results, with shorter columns overestimating leaching potential. Furthermore, columns sampled with mechanical corers showed artificial preferential flow induced by vibration, compromising the representativeness of solute transport. This study highlights the critical role of column design in leaching experiments. By clarifying how these methodological factors influence leaching experiments and DP parameters, this work aims to support the development of standardized practices in soil column leaching research and improve the reliability of contamination risk assessments.

## 1 | Introduction

The intensive use of pesticides in agriculture has significantly degraded the quality of water resources through their leaching. Currently, a large number of pesticides and their metabolites are frequently detected in groundwater, the most important source of drinking water for many European countries [1–4]. Many factors influence the fate of pesticides, such as their properties but also soil characteristics, site conditions, and pesticide application practices. In the last few years, numerous studies have been carried out into the fate of pesticides in soils and the impact of various organic amendments, tillage techniques, and cover crops in order to limit the leaching of these compounds into water [5–8].

Furthermore, numerous modeling tools have been developed to rapidly assess the potential risks associated with the use of pesticides on agricultural land [9–11]. Pesticide transport in soils is primarily governed by adsorption and degradation [12, 13]. Thus, the key input parameters needed for modeling pesticide transport are the sorption coefficient ($K_d$) and the half-life of

the substance ($DT_{50}$). These parameters are usually obtained by inverse modeling of observed data, such as breakthrough curves from field or laboratory experiments [7, 14–16]. In structured soils, preferential flow such as macropores formed by biological activity or mechanical processes (earthworm galleries, cracks) can rapidly transport water and solutes deeper into the soil and increase the risk of water contamination [17, 18]. Many models can be used to consider soil heterogeneity and preferential flows, such as the dual-porosity (DP) approach [7, 19, 20] showed proper modeling of the peaks of several pesticides using DP inverse modeling using Hydrus 1-D.

Long-term field experiments provide realistic conditions, but these are costly, and the parameters are difficult to control due to the high soil heterogeneity and very complex boundary conditions [21]. Laboratory experiments provide relevant information on the potential mobility of pesticides [22]. Soil column leaching experiments are widely used because they provide representations of water and solute fluxes that are closer to the actual field situation. However, studies are carried out at different scales and with a wide range of technical features, which limits comparability between studies, and makes drawing conclusions difficult.

Two types of columns are used to study pesticide leaching: packed and intact soil core columns. Packed columns are made from disturbed soil, which is dried, sieved, and uniformly packed into the column [23–25]. These columns are generally more homogeneous and reproducible than intact core columns. In order to study preferential flows and soil structure, and to get closer to real conditions, a number of studies use intact soil core columns that are directly extracted from the field [6, 7, 26]. Preferential flows through soil macropores significantly reduce the retention of solutes within the soil profile and can therefore increase the risk of groundwater contamination [27]. Sadeghi et al. [28] showed that the packing of soil columns reduces leaching losses of atrazine. In addition, intact soil core columns may contain several soil layers with different properties, which will influence the leaching.

The column sizes used in pesticide leaching experiments vary widely. The diameter of the columns is usually between 8 and 10 cm but can range from 2 to 3 cm to over 50 cm [25, 29, 30]. The length is usually between 20 and 50 cm but shorter columns of 5–20 cm are also very common [14, 24, 29]. From a meta-analysis of 733 soil column tracer leaching experiments, Koestel et al. [31] showed that tracer dispersivity is positively correlated with the length and diameter of the soil column used. Bromly et al. [32] studied the relationship between dispersivity and the properties of 291 disturbed soil columns and concluded that the column diameter was the second most important factor that determines dispersivity after clay content. Furthermore, the degree of preferential flow in intact core columns is positively correlated with the column diameter but negatively correlated with column length.

Several methods of sampling undisturbed soil columns are found in the literature. To avoid sidewall flow, the columns are usually driven directly into the soil. For large soil columns or lysimeters, a static load can be used to drive a heavy steel cylinder into the soil. Another method is to insert a beveled driving head onto a PVC tube and drive it into the ground with a jackhammer or hydraulic pressure system [26, 33]. Smaller columns are usually driven in by hand with a sledgehammer [34]. To sample at deeper depths, drilling equipment can be used to drive columns into the ground. The columns can also be inserted into a steel cylinder of the same size, which is slowly driven into the ground by a mechanical shovel [6].

Thus, varying methodologies can strongly influence the outcome of the experiment [32]. Despite some recommendations by [35] and correlations identified by [31], there remains limited quantitative data on how specific column designs affect solute leaching results. To date, no standardized methodologies exist, and choices regarding sampling methods, soil structure, and column dimensions are often made without clear justification. However, these methodological differences can strongly influence experimental results and lead to irrelevant transport parameters for contamination risk assessment.

The objective of this study is to address these gaps by providing quantitative data on the influence of commonly used soil column methodologies on leaching outcomes within soil columns, as well as on the DP parameters obtained through inverse modeling. Specifically, this research investigates the impact of the following:

- **Soil structure**, by comparing packed and intact soil core columns derived from a silty agricultural soil.
- **Column diameter and height**, using smaller columns of 8.4 cm diameter and larger ones of 24 cm diameter, as well as columns of both 20 and 35 cm in height.
- **Soil layering**, by comparing a 35 cm intact soil core column with a plow sole to a 20 cm homogeneous column. Hydrus 1-D modeling is used to disentangle the effects of column height and soil heterogeneity.
- **Intact core sampling method**, comparing hand-driven columns using a sledgehammer with those inserted via a mechanical auger.

By clarifying how these methodological factors influence leaching experiments and DP parameters, this study aims to support the development of standardized practices in soil column leaching research and improve the reliability of contamination risk assessments.

## 2 | Materials and Methods

### 2.1 | Soils

All soil columns were collected from an agricultural soil located on the Agriculture Is Life experimental plots of the Terra research center of the University of Liege in Gembloux, Belgium. The soil is a cutanic Luvisol according to the World Reference Base for Soil Resources [36]. Its physicochemical properties are given in Table 1. The soil is plowed every year and shows a plow sole below 30 cm. Plowing and sowing of winter wheat were carried out at the end of October 2019 on the plots. The wheat was harvested and stubble was plowed in late July 2020. An intercrop was sown at the beginning of September 2020. The soil was plowed to 30 cm

**TABLE 1** | Physicochemical properties of the soil.

| Properties | 0–30 cm | 30–60 cm |
|---|---|---|
| Collection site | Gembloux, Belgium | |
| Soil type | Luvisol | |
| Texture | Fine silty clay | |
| Clay (%) | 12.0 | 13.1 |
| Silt (%) | 80.5 | 80.5 |
| Sand (%) | 7.5 | 6.4 |
| **Bulk density (g/cm$^3$)** | | |
| - Disturbed | 1.38 ± 0.00 | — |
| - Undisturbed by hand | 1.37 ± 0.02 | 1.4 |
| - Undisturbed by auger | 1.34 ± 0.01 | — |
| pH water | 7.8 | 7.8 |
| Organic carbon (g/kg) | 14.4 | 5.2 |
| Organic matter (%) | 2.9 | 1.0 |
| CEC (meq/100 g) | 10.0 | 8.3 |

and finer work with a rotary harrow at 10 cm depth was done to prepare the seedbed before sowing beet at the end of April 2021. Two hoeing operations were carried out in June 2021. The climate is temperate oceanic, with an average annual temperature of 10.2°C and an average annual rainfall of 837 mm.

## 2.2 | Column Setup

A total of 21 columns were made from Plexiglas tubes. A perforated Plexiglas plate was fixed 2 cm from the bottom of the column in order to elevate it and allow water to pass through. A nylon textile disc was placed between the soil and the perforated plate to prevent soil particles from being washed away. A tube was placed in the water collection area and was connected to two Erlenmeyer flasks and a vacuum pump. All columns were built in triplicate.

### 2.2.1 | Packed Columns

Six packed columns were made with soil taken from 0 to 25 cm depth in June 2020. The soil was first dried at 50°C for 48 h in thin layers before being ground and sieved to 2 mm. The soil was then uniformly packed into the columns to a height of 25 cm, respecting the initial soil density of 1.38 g/cm$^3$. The soil placed in the columns was previously weighed and added in layers of 2–3 cm in height. After each addition, the soil was evenly packed and lightly scarified on the surface to ensure good hydraulic connectivity between the soil layers [37]. Three 8.4 cm columns and three 24 cm internal-diameter columns were reconstituted.

### 2.2.2 | Intact Soil Core Columns

Fifteen intact soil core columns were collected in 8.4 cm diameter Plexiglas tubes from the same agricultural plot as the packed columns. Twelve columns were sampled by hand and driven directly into the field using a sledgehammer and excavated with a shovel and trowel. In early August, three columns were driven to a depth of 25 cm in order to have the same soil height as the packed columns. Subsequently, in early November 2020, three columns were driven in up to 20 cm and three more up to 35 cm to study the impact of the height and the presence of the plow sole. In addition, three columns were sampled to a depth of 30 cm to study the impact of the sampling method in July 2021. Finally, three columns were excavated with a soil column cylinder auger. The soil column auger can be used to sample undisturbed soil columns to a depth of 1 m. The inner diameter of the auger was 90 mm. Thus, a 40 cm long Plexiglas column with an external diameter of 90 mm (84 mm internal diameter) was inserted into the auger before sampling. As the auger is 1 m long, a 60 cm column was placed behind the 40 cm sampling column to hold it in place. The cylinder soil column auger with a cutting head at its base was driven into the ground with a gasoline-powered percussion hammer (Cobra TT) to a depth of 30 cm. The auger was removed from the ground with a steel lifting jack. After removing the detachable lid of the auger, the soil column was carefully removed.

Immediately after excavation, the ends of the columns were sealed in order to bring them to the laboratory without disturbance. To limit possible sidewall flow, paraffin wax was poured on top of the columns at the interface between the soil column and the Plexiglas wall [38, 39]. The columns were kept free of vegetation for the duration of the experiment.

## 2.3 | Leaching Experiment

The leaching experiment modalities are summarized in Table 2. All columns were progressively saturated by adding water above the columns and then allowed to drain freely for 24 h by gravity in order to minimize water content differences at the beginning of the experiment. Saturating the columns from the top may trap air in the soil pore system. This can lead to different hydraulic properties of the soil, such as water retention capacity. This choice was therefore made to more closely simulate field conditions by representing rainfall wetting the soil after a period of drought [40]. All columns were then connected to a peristaltic vacuum pump to provide suction of −35 kPa at the bottom of the column to approximate the real tension conditions [14].

The leaching experiments were performed with a tracer considered to be non-reactive, calcium dichloride (93% purity) from Sigma-Aldrich, USA. A 5 g/L $CaCl_2$ solution was made in a 1 L flask. Then, a 250 mL pulse of solution was added to the 3 columns of 24 cm internal diameter, and a 30.6 mL pulse was added to the 18 columns of 8.4 cm diameter. The same proportion of $CaCl_2$ quantity per soil surface area was respected. The pulse was distributed manually, uniformly over the soil column surface. Then 750 and 91.4 mL of water were added to the 24 and 8.4 cm diameter columns, respectively, to reach 2.2 cm of water.

The $CaCl_2$ leaching experiments were conducted under unsaturated conditions to simulate the situation in the vadose zone and under transient flow to imitate rain events. In fact, intermittent rainfall mimics more natural conditions and can lead to greater

**TABLE 2** | Leaching experiment summary.

| Leaching experiment number | Soil structure | Column diameter (cm) | Column height (cm) | Plow pan | Sampling type | Time of sampling | Agricultural operations |
|---|---|---|---|---|---|---|---|
| 1 + 2 | Disturbed | 8.4 | 25 | No | By hand | June 2020 | |
| 2 | Disturbed | 24 | 25 | No | By hand | June 2020 | |
| 1 | Undisturbed | 8.4 | 25 | No | By hand | August 2020 | Wheat harvested, stubble plowed |
| 3 | Undisturbed | 8.4 | 20 | No | By hand | November 2020 | Intercrops |
| 3 | Undisturbed | 8.4 | 35 | Yes | By hand | November 2020 | Intercrops |
| 4 | Undisturbed | 8.4 | 30 | No | By hand | July 2021 | Soil ploughed, sugar beet planted, soil hoed |
| 4 | Undisturbed | 8.4 | 30 | No | By mechanical auger | July 2021 | Soil plowed, sugar beet planted, soil hoed |

leaching of solutes than steady-flow conditions [41]. After 24 h, 2.2 cm of water was applied onto the columns at a rate of 0.442 cm/min. Similar simulated rainfall was applied to the columns at regular intervals. A surface water layer is built up when water is applied and gradually reduces with the water infiltration into the column. The volume of water percolated and the electrical conductivity of the percolates were measured at regular intervals of 24–48 h. The volume of water percolated was measured in mL with a 250 mL graduated cylinder. The electrical conductivity was measured with a VWR MU1600L multimeter. As the water conductivity is known, the conductivity due to $CaCl_2$ can be obtained. The conductivity was then converted into the $CaCl_2$ concentration using a calibration curve with $CaCl_2$ concentrations of 0, 0.2, 0.4, 0.6, 0.8, and 5 g/L.

## 2.4 | Hydrus 1-D Model

Hydrus 1-D is a one-dimensional finite element model that simulates water, heat, and multiple solute fluxes under various saturation conditions [42]. All breakthrough curves were modeled to derive hydraulic and $CaCl_2$ transport parameters by inverse modeling.

### 2.4.1 | Inverse Modeling

Parameter optimization is an indirect approach for the estimation of water and solute transport parameters from transient flow and transport data. Inverse modeling is based on numerical solutions using the Levenberg–Marquardt (LM) optimization procedure [43]. The LM algorithm minimizes the differences between the observed and simulated values by iteratively adjusting the parameters of interest. This algorithm optimizes the parameters by minimizing the objective function $\varphi(q,b)$ defined by Šimůnek et al. [44]:

$$\Phi(q,b) = \sum_{j=1}^{m} \upsilon_j \sum_{i=1}^{n} w_{ij} \left[ q_j^*(z,t_i) - q_j(z,t_i,b) \right]^2 \quad (1)$$

where $m$ is the number of different sets of measurements, $n$ is the number of observations in a particular measurement set, and $q_j^*(z, t_i)$ are specific measurements at depth $z$ and time $ti$ for the $j$th measurement set, $q_j(z, t_i, b)$ are the corresponding estimated space-time variables for the optimized parameters' vector $b$. $\upsilon_j$ and $w_{ij}$ are weighting factors associated with a particular measurement set or point, respectively.

Three statistical indicators were used to assess the performance of the inverse modeling and parameter optimization: sum of squares (SSQ), root-mean-square error (RMSE), and coefficient of determination ($R^2$). A sequential approach was used, where the hydraulic and transport parameters were estimated successively from the observed water flow data and then from the tracer concentration in the eluates [7, 30, 45]. This approach prevents the uncertainty in the hydraulic parameters from propagating into the uncertainty in the transport parameters [15].

### 2.4.2 | DP Water Flow Modeling

Transient water flows within the columns were simulated using the DP model. Although both single-porosity (SP) and DP formulations were tested, the DP approach was retained for the analysis presented here. A quantitative comparison of the goodness-of-fit between SP and DP models is provided in Tables S1 and S2.

The DP approach considers the porous media to be divided into two interacting regions, partitioning the porous system into mobile and immobile regions. DP models assume that water flow is confined to the macropore or fracture domain. Water in the matrix does not move at all [46, 47]. Water can be exchanged between the two regions. We will use the subscript mo for the mobile or macropore region and im for the immobile region or soil matrix.

The total water content is given by the following equation:

$$\theta = \theta_{mo} + \theta_{im} \quad (2)$$

**TABLE 3** | Hydraulic parameters obtained by Rosetta for the first two layers of the studied soil.

| Column type | Horizon (cm) | $\theta_s$ (–) | $\theta_r$ (–) | $\alpha$ (1/cm) | $n$ (–) | $l$ (–) | $K_s$ (cm/min) |
|---|---|---|---|---|---|---|---|
| Disturbed | 0–30 | 0.4378 | 0.064 | 0.0054 | 1.67 | 0.5 | 0.02139 |
| Undisturbed by hand | 0–30 | 0.4401 | 0.0643 | 0.0053 | 1.6724 | 0.5 | 0.02225 |
| Undisturbed by auger | 0–30 | 0.4471 | 0.0653 | 0.0052 | 1.6791 | 0.5 | 0.02504 |
| — | 30–60 | 0.4374 | 0.0656 | 0.0055 | 1.6601 | 0.5 | 0.01783 |

where $\theta$ is the total soil water content ($L^3/L^3$), and $\theta_{mo}$ and $\theta_{im}$ are the mobile and immobile regions soil water contents, respectively.

In this model, the soil water retention curve $\theta(h)$ is described by the van Genuchten [48] equation, and the hydraulic conductivity function $K(h)$ is described with the statistical pore distribution model of Mualem [49]. These two equations contain five independent hydraulic parameters: the residual soil water content $\theta_r$ ($L^3/L^3$), the saturated soil water content $\theta_s$ ($L^3/L^3$), the hydraulic parameter $n$ (–), the hydraulic shape parameter $\alpha$ (1/L), and the saturated hydraulic conductivity $K_s$ (L/T). The pore connectivity $l$ (–) has been estimated to be 0.5 on average for most soils and set to this value in numerous studies [19, 30, 49, 50]. These parameters were first estimated using neural network-based pedotransfer functions developed by Schaap et al. [51] and incorporated in the Rosetta (Neural Network Predictions) module. The granulometry and bulk density of the soil columns (Table 1) were used. The parameters obtained for Layer 1 of the different column types and for Layer 2 are given in Table 3.

The DP model uses the Richards equation to describe water flow in the mobile region (macropores). A mass balance equation is used to describe water dynamics in the matrix [46]:

$$\frac{\partial \theta_{mo}}{\partial t} = \frac{\partial}{\partial z}\left[K(h)\left(\frac{\partial h}{\partial z} + \cos a\right)\right] - \Gamma_w \tag{3}$$

$$\frac{\partial \theta_{im}}{\partial t} = \Gamma_w \tag{4}$$

where $h$ is the water pressure head (L), $t$ is time (T), $z$ is the vertical coordinate (L), $a$ is the angle between the flow direction and the vertical axis (–), and $\Gamma_w$ is the rate of water transfer from the macropores to the matrix and vice versa (1/T).

The mass transfer rate was assumed to be proportional to the difference in the effective saturations of the two regions using the first-order rate equation [52, 53]:

$$\Gamma_w = \frac{\partial \theta_{im}}{\partial t} = \omega\left[S_e^{mo} - S_e^{im}\right] \tag{5}$$

where $\omega$ is the first-order rate coefficient for water transfer between mobile and immobile regions (1/T), and $S_e{}^{mo}$ and $S_e{}^{im}$ are the effective fluid saturations of the mobile (macropores) and immobile (matrix) regions.

The retention curves are considered by the model to be similar for both regions. The parameters $\alpha$ and $n$ of the van Genuchten equation therefore have the same value for both regions [18, 41].

For the mobile region (macropores), the parameters required by the model are $\theta_{r,mo}$, $\theta_{s,mo}$, $\alpha$, $n$, and $K_s$. For the immobile region (matrix) the parameters are $\theta_{r,im}$, $\theta_{s,im}$, and $\omega$.

The initial values of the parameters $a$, $n$, and $K_s$ are the ones given by the Rosetta module. The parameters $\theta_{s,mo}$ and $\theta_{s,im}$ are calculated assuming a proportion of macropores of 10% of the total calculated soil porosity. Thus, $\theta_{s,mo}$ is equal to 0.1 of $\theta_s$, and $\theta_{s,im}$ to 0.9 of $\theta_s$ [54, 55]. $\theta_{r,im}$ is assumed to be equal to the $\theta_r$ value of the soil obtained from the Rosetta module. $\theta_{r,mo}$ is set to zero to ensure that residual water is only present in the immobile zone of the soil [19, 30]. The first-order rate coefficient for water transfer $\omega$ was set to 0.002 1/min [56]. The parameters $\theta_{s,mo}$, $K_s$, and $\omega$ were optimized by inverse modeling of the cumulative flow measurements for each column. Then $\theta_{s,im}$ was calculated according to Equation (2). Mertens et al. [57] showed that saturated hydraulic conductivity ($K_s$) was the most sensitive parameter when inverse modeling was performed using eluted water volume data. In order to separate the effect of the height of the columns and the presence of a plow sole, the 35 cm columns were modeled by first considering a single 35 cm horizon "35(1H)" and then considering the two horizons separately with the first 30 cm and then the last 5 cm of the plow sole "35(2H)". For 35 cm columns with two horizons, the parameters of both layers are optimized simultaneously.

### 2.4.3 | DP Solute Transport Modeling

The transport of a tracer in a porous medium with variable saturation is described by the classical convection-dispersion equation where no tracer adsorption or degradation occur [58]:

$$\frac{\partial \theta_{mo} c_{mo}}{\partial t} = \frac{\partial}{\partial x}\left(\theta_{mo} D_{mo} \frac{\partial c_{mo}}{\partial x}\right) - \frac{\partial q_{mo} c_{mo}}{\partial x} - \Gamma_s \tag{6}$$

$$\frac{\partial \theta_{im} c_{im}}{\partial t} = \Gamma_s \tag{7}$$

$$\Gamma_s = \omega_s\left(c_{mo} - c_{im}\right) + \Gamma_w c^* \tag{8}$$

In which, $c_{mo}$ and $c_{im}$ are the solute liquid concentrations of the mobile and immobile regions ($M/L^3$), $D_{mo}$ is the dispersion coefficient in the mobile region, taking into account molecular diffusion and hydrodynamic dispersion ($L^2/T$), $q_{mo}$ is the volumetric flux density in the mobile region (L/T), $\Gamma_s$ is the solute transfer rate between the two regions ($M/L^3T$). $\omega_s$ is the first-

order chemical mass transfer coefficient (1/T), and $c^*$ is the solute concentration (M/L$^3$) of the mobile region $c_{mo}$ for $\Gamma_w > 0$ and of the immobile region $c_{im}$ for $\Gamma_w < 0$ [58].

The dispersion coefficient of the mobile zone $D_{mo}$ can be described as

$$D_{mo} = D_0 \frac{\theta_{mo}^{\frac{7}{3}}}{\theta_{s,mo}^2} + \lambda_{mo} v \quad (9)$$

where $D_0$ is the molecular diffusion coefficient in free water (L$^2$/T), $\lambda_{mo}$ is the longitudinal dispersivity in the mobile region (L), and $v$ is the pore water velocity (L/T).

Dispersivity $\lambda$, molecular diffusion coefficient $D_0$ and first-order chemical mass transfer coefficient $\omega_s$ are required. The dispersivity value is usually set at 1/10 of the column size [55]. Thus, for 20 and 35 cm columns, an initial dispersivity of 2 and 3.5 cm, respectively, is considered. The diffusion coefficient ($D_0$) is mostly of the order of 5% of the hydrodynamic dispersion coefficient [59]. The molecular diffusion coefficient of $CaCl_2$ is 0.0008 cm$^2$/min [60]. The initial value of the transfer coefficient $\omega_s$ has been set to 0.00001 1/min [55].

Finally, the observed $CaCl_2$ concentration data in the leachate were used for optimization by inverse modeling the values of $\lambda$, $D_0$, and $\omega_s$ [45, 61]. For the 35 cm columns considering two horizons, the parameters of the first layer were adjusted first and then those of the second layer.

#### 2.4.4 | Boundary Conditions

For the numerical modeling with Hydrus 1-D, columns were represented as 1-D domains and discretized into 101 nodes with equal spacing. The water flow boundary condition was defined on top of the soil column as atmospheric boundary conditions with a surface water layer to allow for water buildup during time-variable boundary conditions of water addition (precipitation). Thus, a flow rate of 0.442 cm/min for 5 min was set as a variable boundary condition at each water addition. At the bottom, the water flow boundary condition was set to constant pressure head because the vacuum pump connected to the bottom of the column induces a constant tension of −35 kPa. The solute transport boundary condition at the top of the column is a concentration flux with $CaCl_2$ applied at a concentration of 5 g/L. At the bottom of the column, a zero-concentration gradient is defined.

### 2.5 | Data Treatment and Statistical Analysis

Breakthrough curves were constructed using the relative concentrations ($C/C_0$) measured in the leachates over the cumulative relative pore volume ($V/V_0$). The porosity was calculated from the average bulk density for each column type (disturbed, undisturbed sampled by hand; and undisturbed sampled with a mechanical auger) and the density of the soil particles and organic matter. Assuming a soil particle density of 2.65 g/cm$^3$ and an organic matter particle density of 1.4 g/cm$^3$, the particle density of the whole soil was found to be 2.614 g/cm$^3$ (Table 1).

Data were processed using RStudio v2023.12.0. The figures were plotted with ggplot2 package. The $T_{min}$, $C_{peak}$, and $T_{peak}$ indicators were determined as the relative pore volume at the first appearance of the tracer in the eluates, the maximum relative concentration, and the relative pore volume after which it was reached for each column.

To investigate the existing differences between the breakthrough curves of several soil column designs and transport parameters, analyses of variance (ANOVA) were performed. In order to compare the means of several indicators of the breakthrough curves and of DP parameters, Fisher's least significant difference (LSD) method was used with the null hypothesis of equality of means and a significance level of 0.05. Normality was tested using Shapiro–Wilk and equality of variances using Levene's test. All assumptions were satisfied.

## 3 | Results and Discussion

### 3.1 | Soil Structure

Figure 1 represents the comparison of $CaCl_2$ breakthrough curves for the packed, disturbed columns of 24 and 8.4 cm diameter and intact soil core columns of 8.4 cm diameter (leaching experiment no. 1 and 2).

The arrival times of the first breakthrough $T_{min}$, the arrival time of the maximal peak concentration $T_{peak}$, the relative maximal concentration of the peak $C_{peak}$, and the total pore volume eluted $T_{tot}$ for the tracer $CaCl_2$ for the four leaching experiments are given in Table 4.

Breakthrough curves show different patterns between the two soil structures (disturbed and undisturbed). The solute is found faster in the leachates with a significantly lower time ($p$ value = 0.002) of first breakthrough ($T_{min}$) for the undisturbed column than for the disturbed column, where it is more retained. The peak (arrival time of the maximal peak concentration $T_{peak}$) also appeared faster for intact soil core columns than for the packed column, indicating greater retention of the solute in the disturbed soil structure.

Soil structure also influences the height and width of the breakthrough curve. The maximal concentration of the peak ($C_{peak}$) is significantly higher ($p$ value = 0.0001) for the disturbed columns. Furthermore, the total amount of pore volume required to complete the pulse was significantly lower ($p$ value = 0.001) for packed columns with an average value of 1.205 ± 0.098 than for intact soil core columns at 1.626 ± 0.096. The breakthrough curves of packed columns show a $T_{peak}$ that is 1.41 times higher, a $C_{peak}$ (height) 1.95 times higher, and a pore volume required to complete the pulse (width) 1.35 times lower than the intact columns.

The percentage of $CaCl_2$ recovered is higher ($p$ value = 0.002) for the disturbed columns than for the intact columns (Table 5). For the disturbed columns, an estimated percentage of $CaCl_2$ recovered exceeding 100 is obtained as a result of the electrical

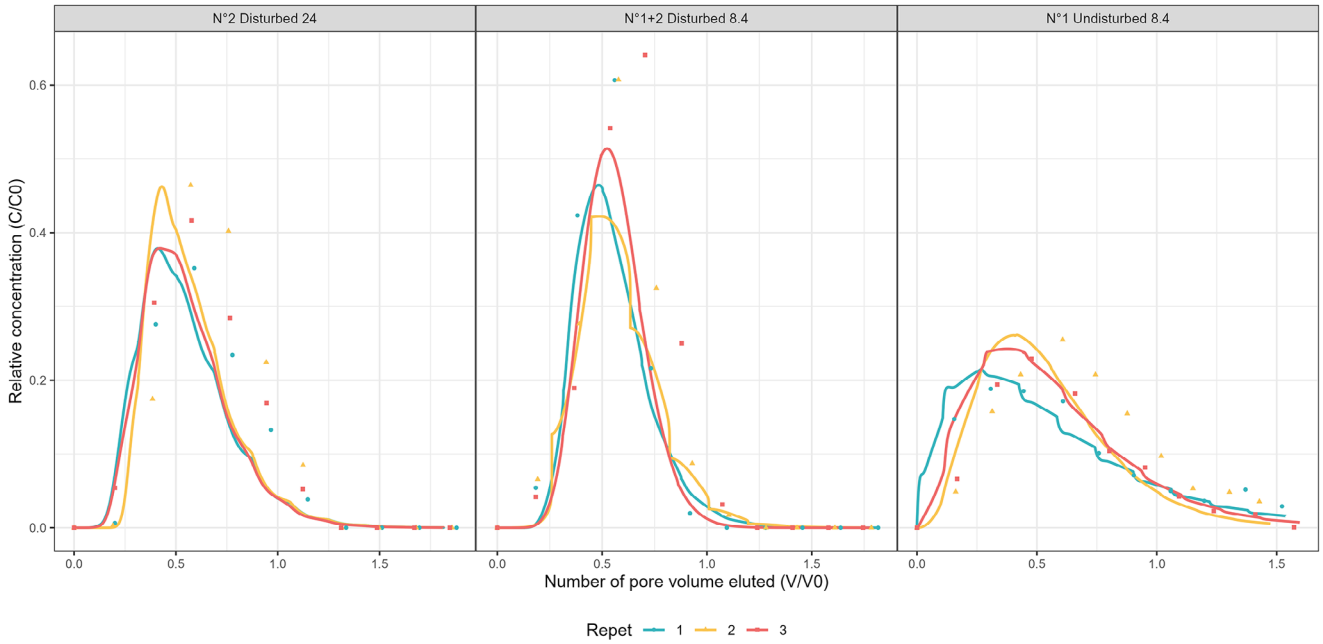


**FIGURE 1** | Measured and modeled breakthrough curves depicting the relative concentration ($C/C_0$) in the leachates plotted as a function of the number of pore volume eluted ($V/V_0$) for the $CaCl_2$ tracer: (a) for disturbed columns of 24 cm diameter, (b) disturbed columns of 8.4 cm diameter, and (c) undisturbed columns of 8.4 cm diameter for the three replicates. The points correspond to the measured and the lines to the modeled data.

**TABLE 4** | Arrival time of the first breakthrough $T_{min}$ in pore volume, arrival time of the maximum peak concentration $T_{peak}$ in pore volume, relative maximal peak concentration $C_{peak}$, and total pore volume eluted $T_{tot}$ for the four leaching experiments.

| Columns | $T_{min}$ | $T_{peak}$ | $C_{peak}$ | $T_{tot}$ |
|---|---|---|---|---|
| R24 | 0.135 ± 0.046 | 0.421 ± 0.008 | 0.407 ± 0.040 | 1.86 ± 0.01 |
| R8.4 | 0.152 ± 0.011 | 0.499 ± 0.018 | 0.467 ± 0.0038 | 1.78 ± 0.03 |
| U8.4 | 0.010 ± 0.010 | 0.353 ± 0.064 | 0.240 ± 0.019 | 1.51 ± 0.06 |
| **20** | **0.001 ± 0.001** | **0.119 ± 0.025** | **0.492 ± 0.022** | **1.66 ± 0.03** |
| **35** | **0.003 ± 0.001** | **0.045 ± 0.021** | **0,397 ± 0.021** | **0.88 ± 0.05** |
| Hand | 0.021 ± 0.013 | 0.238 ± 0.091 | 0.261 ± 0.075 | 0.78 ± 0.06 |
| Auger | 0.002 ± 0.000 | 0.049 ± 0.028 | 0.516 ± 0.067 | 1.03 ± 0.08 |

*Note:* Values correspond to the mean of the three spatial replicates with standard deviation.

**TABLE 5** | Percentage of $CaCl_2$ recovered for all the soil columns studied.

| Leaching experiment number | Soil material | Column diameter (cm) | Column height (cm) | Sampling type | % $CaCl_2$ recovered (mean) | % $CaCl_2$ recovered (standard deviation) |
|---|---|---|---|---|---|---|
| 1 + 2 | Disturbed | 8.4 | 25 | By hand | 141.5 | 13.4 |
| 2 | Disturbed | 24 | 25 | By hand | 123.0 | 15.0 |
| 1 | Undisturbed | 8.4 | 25 | By hand | 87.4 | 9.5 |
| 3 | Undisturbed | 8.4 | 20 | By hand | 67.4 | 2.2 |
| 3 | Undisturbed | 8.4 | 35 | By hand | 41.0 | 2.7 |
| 4 | Undisturbed | 8.4 | 30 | By hand | 63.2 | 17.0 |
| 4 | Undisturbed | 8.4 | 30 | By mechanical auger | 91.4 | 7.4 |

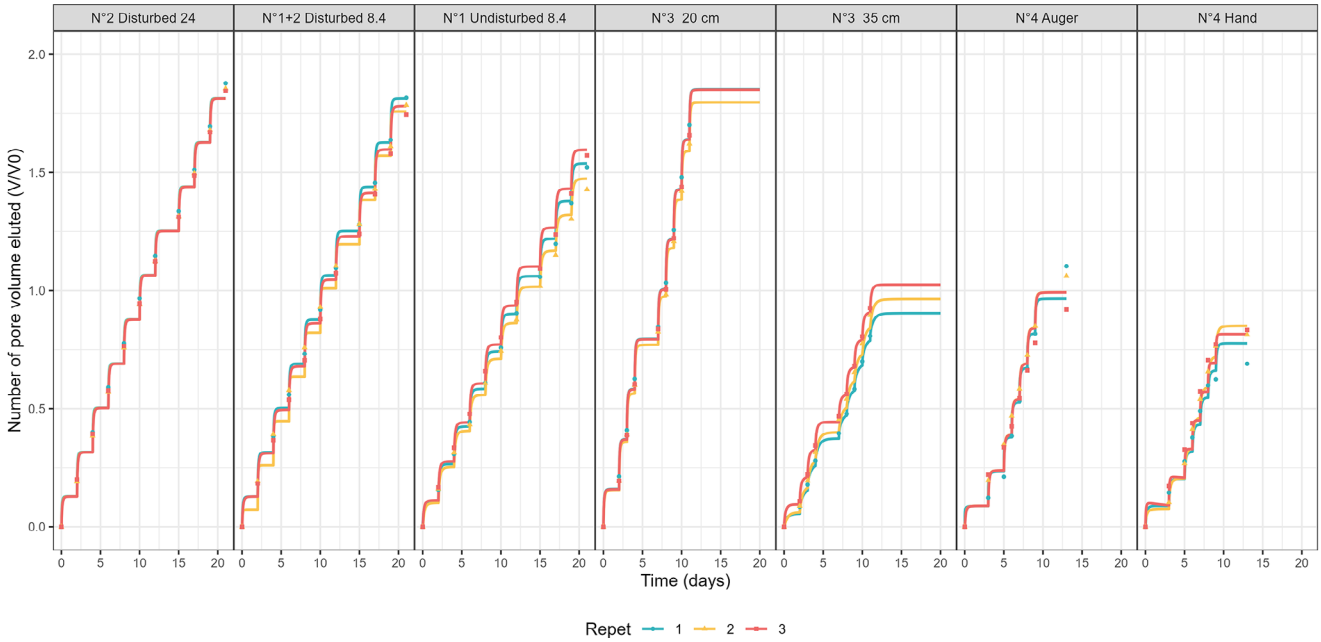


**FIGURE 2** | Measured and modeled cumulative outflow curves depicting the number of pore volume eluted ($V/V_0$) plotted as a function of the time (in days) since the pulse, for (a) disturbed column of 24 cm diameter, (b) disturbed column of 8.4 cm diameter, (c) undisturbed column of 8.4 cm diameter, (d) undisturbed column of 20 cm height, (e) undisturbed column of 35 cm height, (f) undisturbed column collected with the soil column cylinder auger, and (g) undisturbed column collected by hand for the three replicates. The points correspond to the measured and the lines to the modeled data.

**TABLE 6** | Soil hydraulics parameters obtained by inverse modeling of cumulative outflow.

| Columns | $\theta_{s,mo}$ ($cm^3/cm^3$) | $\theta_{s,im}$ ($cm^3/cm^3$) | Proportion of the mobile zone (%) | $K_s$ (cm/min) | $\omega$ (1/min) | SSQ (–) | $R^2$ (–) |
|---|---|---|---|---|---|---|---|
| R24 | 0.35 ± 0.01 | 0.13 ± 0.01 | 74.3 ± 1.3 | 0.105 ± 0.017 | 0.049 ± 0.021 | 0.02 ± 0.00 | 1.00 ± 0.00 |
| R8.4 | 0.29 ± 0.02 | 0.19 ± 0.02 | 60.6 ± 4.9 | 0.095 ± 0.013 | 0.041 ± 0.040 | 0.01 ± 0.00 | 1.00 ± 0.00 |
| U8.4 | 0.24 ± 0.03 | 0.23 ± 0.03 | 51.0 ± 5.4 | 0.056 ± 0.008 | 0.01 ± 0.004 | 0.01 ± 0.00 | 1.00 ± 0.00 |
| **20** | **0.21 ± 0.03** | **0.26 ± 0.03** | **43.8 ± 6.7** | **0.060 ± 0.002** | **0.028 ± 0.009** | **0.00 ± 0.00** | **1.00 ± 0.00** |
| **35 (1H)** | **0.17 ± 0.03** | **0.31 ± 0.03** | **35.3 ± 5.3** | **0.080 ± 0.004** | **0.000 ± 0.000** | **0.00 ± 0.00** | **1.00 ± 0.00** |
| | **0.18 ± 0.01** | **0.29 ± 0.01** | **38.3 ± 2.2** | **0.074 ± 0.005** | **0.003 ± 0.004** | | |
| **35 (2H)** | **0.06 ± 0.02** | **0.38 ± 0.02** | **12.9 ± 3.5** | **0.023 ± 0.005** | **0.000 ± 0.000** | **0.00 ± 0.00** | **1.00 ± 0.00** |
| Hand | 0.21 ± 0.02 | 0.26 ± 0.02 | 44.4 ± 5.0 | 0.058 ± 0.012 | 0.001 ± 0.001 | 0.093 ± 0.05 | 0.99 ± 0.01 |
| Auger | 0.17 ± 0.00 | 0.32 ± 0.00 | 34.9 ± 0.5 | 0.112 ± 0.008 | 0.023 ± 0.002 | 0.06 ± 0.04 | 0.99 ± 0.01 |

*Note:* Values correspond to the mean value of the three spatial replicates with the standard deviation. The terms 35 (1H) refer to modeling considering a single soil layer of 35 cm and 35 (2H) to modeling considering a first layer of 30 cm and then the plow pan of 5 cm separately.

conductivity conversion to concentration. Soil disturbance may have resulted in the leaching of other solutes than the $CaCl_2$, previously retained within the soil matrix.

Very good agreement was achieved between observed and predicted cumulative outflow (Figure 2).

The average $R^2$ of the water flux modeling is 1.00 ± 0.00 for the disturbed columns and 1.00 ± 0.00 for the undisturbed columns (Table 6). The $K_s$ values for packed columns are on average significantly higher ($p$ value = 0.000) compared to intact soil core columns. In this way, the long tail of the intact columns' curves may be due to a higher degree of solute transport in low flow regions. Thus, water infiltration is slower at saturation for the undisturbed columns. The proportion of the mobile region is also greater for disturbed columns than for columns in undisturbed structure.

The transport parameters fitting resulted in a proper representation of solute transport with an average $R^2$ of 0.89 ± 0.06 for the disturbed columns and 0.92 ± 0.07 for the undisturbed columns (Table 7). The dispersivity values obtained for the

**TABLE 7** | Fitted transport parameters determined by inverse modeling of leachate concentrations on Hydrus 1-D.

| Columns | $\lambda$ (cm) | $D_0$ (cm$^2$/min) | $\omega_s$ (1/min) | SSQ | $R^2$ |
|---|---|---|---|---|---|
| R24 | 0.29 ± 0.10 | 0.000 ± 0.000 | 0.001 ± 0.000 | 0.12 ± 0.10 | 0.95 ± 0.04 |
| R8.4 | 0.24 ± 0.07 | 0.009 ± 0.010 | 0.037 ± 0.022 | 0.24 ± 0.05 | 0.89 ± 0.06 |
| U8.4 | 2.89 ± 1.20 | 0.002 ± 0.000 | 0.005 ± 0.003 | 0.15 ± 0.15 | 0.92 ± 0.07 |
| **20** | **3.48 ± 1.36** | **0.002 ± 0.003** | **0.000 ± 0.000** | **0.12 ± 0.07** | **0.90 ± 0.05** |
| **35 (1H)** | **22.6 ± 1.66** | **0.002 ± 0.002** | **0.000 ± 0.000** | **0.26 ± 0.06** | **0.80 ± 0.02** |
| | **17.1 ± 6.73** | **0.001 ± 0.000** | **0.000 ± 0.000** | | |
| **35 (2H)** | **0.24 ± 0.01** | **0.001 ± 0.000** | **0.000 ± 0.000** | **0.28 ± 0.04** | **0.78 ± 0.04** |
| Hand | 1.42 ± 0.70 | 0.001 ± 0.001 | 0.001 ± 0.001 | 0.27 ± 0.21 | 0.84 ± 0.12 |
| Auger | 33.44 ± 7.84 | 0.000 ± 0.000 | 0.000 ± 0.000 | 0.14 ± 0.05 | 0.93 ± 0.06 |

*Note:* Values correspond to the mean value of the three spatial replicates with the standard deviation. The terms 35 (1H) refer to modeling considering a single soil layer of 35 cm and 35 (2H) to modeling considering a first layer of 30 cm and then the plow pan of 5 cm separately.

undisturbed columns were on average significantly higher ($p$ value = 0.009) at 2.89 ± 1.20 cm compared to 0.24 ± 0.07 cm for the disturbed columns. The dispersivity values were smaller than 1 for all the disturbed columns, indicating very low spatial heterogeneity in these columns. The diffusion coefficient shows no significant difference between the two structures. The mass transfer coefficient $\omega_s$ was significantly higher for disturbed columns than for intact columns. Thus, the dispersion is 12.3 times greater, and the tracer mass transfer is 26.5 times lower for intact soil cores than for disturbed columns.

The results show that soil structure significantly affects the dynamics of water infiltration and solute transport. The $CaCl_2$ breakthrough curves reveal markedly different transport patterns between disturbed and intact columns. They are symmetrical for the packed columns, whereas they are asymmetrically shifted to the left with a generally longer tailing for the intact soil core columns, as observed by Kamra et al. [62] and Singh et al. [63].

In the disturbed columns, water and solute pass through a homogeneous soil matrix with a uniform flow, resulting in a gradual increase and decrease in solute concentration in the leachate. The solute is retained for longer, and all the solute comes out at the same time, generating a higher $C_{peak}$. Higher $K_s$ values in disturbed columns suggest that soil reorganization favors more homogeneous and faster flow. Celestino Ladu and Zhang [64] also found a greater water velocity, from 2 to 10 times greater for the undisturbed columns than for the disturbed columns. However, during the column saturation, air bubbles may have been trapped, limiting the passage of water through some pores.

The asymmetry and the long tailing of the intact soil core curves for a tracer indicate the presence of physical nonequilibrium transport processes [26, 62, 65]. Transport is faster in intact columns, with the arrival of the tracer ($T_{min}$) and the peak of maximum concentration ($T_{peak}$) coming earlier. The acceleration of tracer transport results from a greater degree of preferential flows through macropores. These preferential flows are generated by earthworm galleries, root holes, and soil cracks. The greater dispersivity of the tracer in the undisturbed columns shows the greater degree of preferential flow in these columns, in contrast to the very low dispersivity of the disturbed columns [27]. A greater dispersivity of a solute within intact columns than in disturbed columns has also been observed by [66]; Koestel et al. [31] showed that moderate to strong preferential flows are found only in soils with more than 8%–9% clay. The percentage of clay being 12 in the studied soil and the presence of moderate 220 to strong preferential flows having an impact on the breakthrough curve shape is consistent. The first replicate of the intact soil core shows faster tracer transport than the other two replicates, as indicated by the breakthrough curve being shifted to the left. $T_{peak}$ occurs earlier (0.26 PV compared to 0.42 and 0.38 PV for replicates 2 and 3). Greater dispersivity is also obtained (4.56 compared to 1.82 and 2.28 after the other two repetitions) with a lower mass transfer coefficient (0.01 compared to 0.007 and 0.006 1/min). Thus, this column shows a degree of preferential flow with more pronounced physical nonequilibrium processes. As the proportion of the mobile zone is similar in all three replicates, the macropores may be more connected in this column. This difference between the three replicates shows the heterogeneity of the columns taken directly in the field.

Moreover, the solute in the soil matrix is considered immobile. The solute mass transfer coefficient between the mobile and immobile regions is lower in the intact soil core, which may explain their longer retention and the lower mass recovered. Some of the water passes through the macropores and therefore does not contribute significantly to the transport of solute that has diffused into the soil matrix [67]. In intact columns, the lower recovery is consistent with dispersion in the soil matrix and partial trapping of the solute in the immobile region. The tracer will emerge at different times depending on the traveled path, resulting in a more gradual elution. Greater solute retention was also observed with lower $C_{peak}$ and more widespread breakthrough curves. The widespread is also an indication of the heterogeneity of soil transport processes [33]. Stubble plowing was carried out 2 weeks before the undisturbed columns were sampled. This operation disrupted the surface structure, limiting the continuity of the macropores along the entire length of the columns.

These results confirm that soil structure has a strong influence on solute transport dynamics and therefore on the assessment of the risk of groundwater contamination. Natural soils exhibit complex transport dynamics, with a fraction of the contaminant migrating rapidly through macropores, while another fraction remains trapped in the soil matrix. The use of disturbed columns can lead to a poor assessment of the leaching potential of contaminants under real conditions. Neglecting these preferential flows can lead to an underestimation of the risk of rapid contamination for highly mobile pollutants and an overestimation of the biodegradation or sorption of certain contaminants due to an interaction with the soil matrix that may be less significant in real conditions. Our research shows that the study of water and solute fluxes in disturbed columns does not provide a suitable representation of the risk of groundwater contamination. The differences between the two types of columns are very pronounced in terms of the breakthrough curves and transport parameters obtained by Hydrus 1-D. Therefore, in order to better approximate real field conditions, intact columns are recommended to assess solute transport. Soil column experiments are an essential tool for modeling contaminant transport, but their design must be rigorously adapted to the objectives of the study. Accounting for soil heterogeneity and preferential transport is essential to improve the reliability of contaminant transfer models and to optimize environmental management strategies.

### 3.2 | Column Diameter

The diameter of a disturbed column has only a minor influence on the shape of the $CaCl_2$ breakthrough curves (leaching experiment no. 2). Both the 24 and 8.4 cm diameter columns displayed symmetrical curves with similar elution patterns (Figure 1).

The solute is detected at the same time ($p$ value = 0.573) in the leachates with a similar $T_{min}$ between the 8.4 and 24 cm diameter columns. Peak positions also aligned closely, with maximum $CaCl_2$ concentrations being reached after similar pore volumes ($p$ value = 0.092). Given that the soil in both columns was sieved to 2 mm and reconstructed to the same bulk density (1.38 g/cm$^3$), the transport velocity of solutes was expected to be uniform. Additionally, the travel distance for solute elution was identical at 25 cm for both column types, reinforcing the observed similarity in transport dynamics. Thus, the majority of the solute will emerge after a similar eluted pore volume.

The column diameter does not affect the height or the width of the curves. The maximum relative concentrations $C_{peak}$ and the total pore volume required to complete the pulse were not significantly ($p$ value = 0.121) different for the 24 cm and the 8.4 cm columns.

Very good agreement was achieved between observed and predicted cumulative outflow. The average $R^2$ of the water flux modeling is 1.00 ± 0.00 for the disturbed columns (Table 6). The $K_s$ values are, on average, not significantly different ($p$ value = 0.240) between the two diameters. However, the proportion of the mobile zone is higher for disturbed columns of 24 cm ($p$ value = 0.006) with 74.3% compared to columns of 8.4 cm with 60.6%. This suggests that the larger columns allowed for greater preferential flow or enhanced water movement through mobile zones.

Transport parameter fitting resulted in a satisfactory representation of solute transport with an average $R^2$ of 0.95 ± 0.04 for the 24 cm diameter disturbed columns and 0.89 ± 0.06 for the 8.4 cm diameter columns (Table 7). The average dispersivity values obtained for the 24 and 8.4 cm diameter columns were not significantly different ($p$ value = 0.940). Dispersivity values were lower than 1 for all disturbed columns, indicating very low spatial heterogeneity in these columns. These results contrast with findings from Vanderborght and Vereecken [59] and Bromly et al. [32], who observed that dispersivity increases with larger lateral scales. This discrepancy is likely due to the disturbed nature of the soil structure in our experiments, which minimized lateral redistribution and dispersion, as highlighted by Koestel et al. [31]. A higher dispersivity typically reduces solute peak concentrations and smooths concentration gradients [59].

The results show that for disturbed soil columns, the diameter has only a limited impact on the $CaCl_2$ breakthrough curves and measured transport parameters. This similarity can be attributed to the homogeneous soil matrix across all columns. However, as highlighted in the previous section, disturbed soil columns do not adequately represent water and solute flows in natural soils, where structure plays a critical role. Thus, although column diameter has minimal influence on results obtained from homogenized soils, these results may differ significantly for columns with preserved structure. Therefore, although small-diameter columns can be sufficient for experiments that require disturbed soil columns, they may not be appropriate for assessing solute transport in structured soils.

### 3.3 | Column Height and Differentiated Layers

Figure 3 shows the comparison of the $CaCl_2$ breakthrough curves for the 20 and 35 cm undisturbed columns. The 35 cm column includes 5 cm of plow sole between 30 and 35 cm (leaching experiment no. 3). It should be noted that the comparison between the 20 and 35 cm columns inherently combines two factors: an increase in column height and the inclusion of a differentiated plow sole in the lower part of the 35 cm column. This coupling constitutes a limitation of the experimental design. However, this configuration reflects real field conditions, as the studied soil systematically exhibits a compacted layer below 30 cm depth.

The height of the intact soil cores significantly influences the shape of the $CaCl_2$ breakthrough curves (Figure 3). All curves show pronounced asymmetry with long tails, indicating the presence of preferential flow pathways. Although solutes are detected at similar $T_{min}$ values in the leachate for both the 20 and 35 cm columns ($p$ value = 0.128), the peak positions differ. The maximum $CaCl_2$ concentrations are obtained after an average pore volume that was significantly higher ($p$ value = 0.003) for the 20 cm columns than for the 35 cm columns. The majority of the solute is eluted with the first few pore volumes of water for all columns, indicating the probable presence of continuous macropores throughout the columns. The peak position difference results from a greater pore volume in the 35 cm than in the 20 cm columns. Strong preferential flows within the columns resulted in rapid elution of solute, which may have overshadowed the real effect of height and the presence of a differentiated horizon on

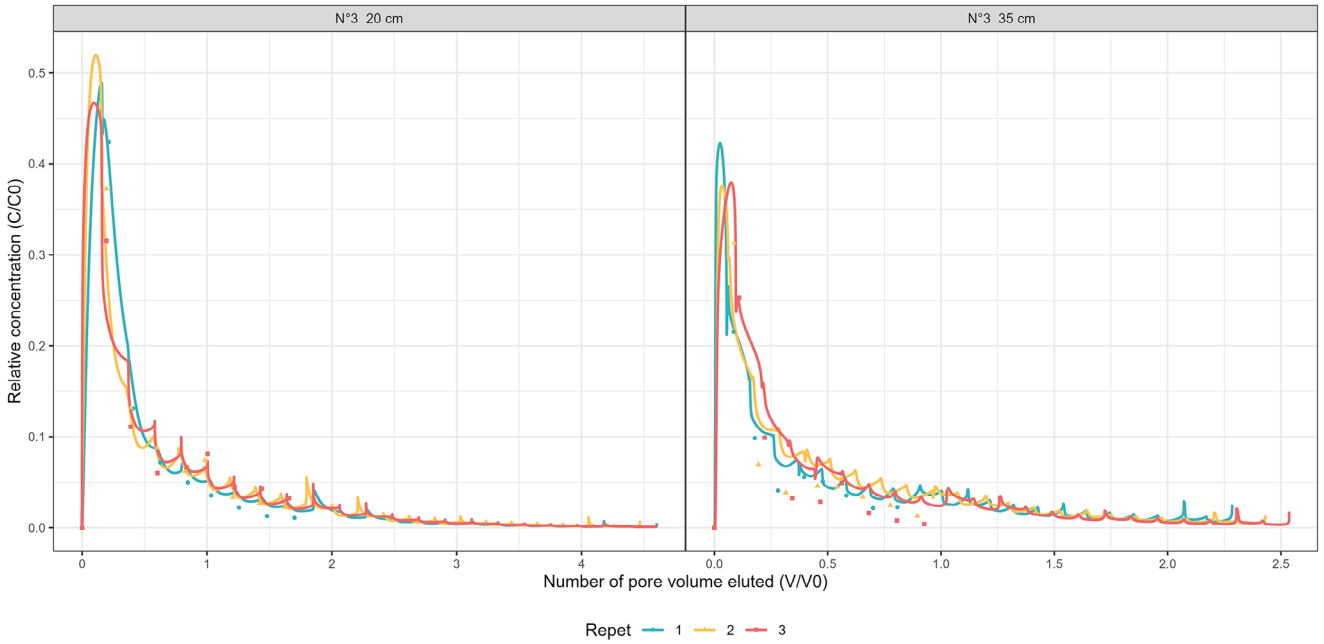


**FIGURE 3** | Measured and modeled breakthrough curves depicting the relative concentration ($C/C_0$) in the leachates plotted as a function of the number of pore volume eluted ($V/V_0$) for the $CaCl_2$ tracer, (a) for undisturbed columns of 20 cm height and (b) for undisturbed columns of 35 cm height for the three replicates. The points correspond to the measured and the lines to the modeled data.

the shape and the position of the peak [6]. In comparison, the peak position of the intact 25 cm columns performed for leaching experiment no. 1 just after stubble plowing is, on average, higher. The greater asymmetry of the breakthrough curve compared to the intact columns in leaching experiment no. 1 carried out just after harvesting and stubble plowing is due to the greater importance of preferential flows. These columns were made in November, 2 months after an intercrop was planted, leading to the formation of aggregates and macropores mainly due to earthworm burrows and root holes. Stronger preferential fluxes are observed in soils with higher aggregate stability and greater soil structure [68]. In addition, Koestel et al. [31] showed that moderate-to-strong preferential flows are found only in soils with more than 8%–9% clay, and the percentage of clay in the studied soil is 12. This highlights the dynamic of soil structure development, influenced by the timing of sampling and crop management practices.

The column height and the presence of a differentiated horizon significantly influence the height and the width of the breakthrough curve. The maximum relative concentrations of $CaCl_2$ tracer were significantly higher for the 20 cm columns ($p$ value = 0.01), with a greater amount of $CaCl_2$ recovered (67.4% ± 2.2% compared to 41.0% ± 2.7% for the 35 cm columns; $p$ value = 0.0001). The total pore volume $T_{tot}$ was significantly higher ($p$ value = 0.0001) for the 20 cm columns than for the 35 cm columns. Thus, the breakthrough curves of the 20 cm columns show a maximum relative concentration 1.3 times higher, with an amount of $CaCl_2$ recovered 1.6 times higher for a pore volume to complete the pulse 1.9 times higher than the 35 cm columns.

Regarding the optimized values of water transport, the average $R^2$ is 1.00 ± 0.00, indicating the high accuracy of the water fluxes represented by the model. The modeling differentiated between the 20 cm columns, the 35 cm columns with a single horizon, and the 35 cm columns with two horizons (30 cm + 5 cm plow sole). Although the mobile zone proportion was similar between the 20 cm columns and the upper 30 cm of the 35 cm columns, it was significantly reduced (12.9%, $p$ value = 0.0001) within the plow sole. This suggests limited solute mobility in compacted layers, potentially leading to solute retention.

The values of $K_s$ for the 20 cm columns are on average similar to the first 30 cm of the 35 cm columns ($p$ value = 0.122). These values are higher than the value of 0.022 cm/min initially estimated by Rosetta. Strong preferential flows will result in a rapid water flow, and the model increases the $K_s$. The plow sole has lower conductivity with an average of 0.023 ± 0.005 cm/min, closer to the initial value.

The fitted transport parameters resulted in an appropriate representation of the transport of the solute with an average $R^2$ of 0.90 ± 0.05 for the 20 cm columns, 0.80 ± 0.02 for the 35 cm columns with one horizon and 0.78 ± 0.04 with two horizons (Table 7). The alternating increases and decreases in concentration observed in the breakthrough curves may be due to the dynamics of mass exchange between the mobile region of the macropores and the immobile region of the soil matrix. This mass exchange between the two regions can play an important role in solute leaching. During periods without rainfall, the local solute concentration will gradually approach equilibrium through diffusive exchanges of the solute from the matrix region to the macropores. Following rainfall, the solutes present in the macropores can create another peak in the breakthrough curve [41]. The dispersivity values obtained for the 20 cm columns were on average significantly lower ($p$ value = 0.001) compared to the horizon 1 of 35 cm columns or to the whole 35 cm columns (1H). Thus, 35 cm columns exhibit a dispersivity 6.5 times greater than

20 cm columns. The dispersivity values were smaller than 1 for the plow sole. The highest dispersivity values for the 35 cm columns show greater soil heterogeneity and higher preferential flows [27]; Vanderborght et al. [59] and Koestel et al. [31] demonstrated that apparent dispersivity is positively correlated with travel distance, which is consistent with our findings. In addition, the solute may have been retained in the column for a longer time by the plow pan. However, no significant difference was observed between the first 30 cm (horizon 1) and the entire 35 cm column. Interestingly, despite the presence of the plow sole, layered Hydrus 1-D modeling suggests that the observed differences in transport behavior between the 20 and 35 cm columns are primarily due to the increased soil column height. Although the plow sole locally reduces hydraulic conductivity and solute mobility, its influence is secondary compared to the effects of travel distance and dispersivity at the column scale. The differences in pore volume and solute dispersivity in the 35 cm columns contributed to lower $CaCl_2$ recovery and reduced peak concentrations in the leachate.

The timing of sampling in relation to cultivation operations appears to influence the solute leaching through the soil profile. Compared to the intact columns of leaching experiment no. 1 performed just after a stubble plowing that disturbed the topsoil, the solute peak arrives after a pore volume 3.0 times higher, the maximum peak concentration is 2 times lower, and the dispersivity is 1.2 times lower than for the 20 cm height columns. This demonstrates how soil structure evolves over time, with macropore formation and aggregation increasing preferential flow pathways and solute mobility.

Our study showed significant differences in breakthrough curves and transport parameters between the 20- and 35-cm columns. However, in structured agricultural soils, column height effects cannot be fully disentangled from soil heterogeneity, particularly when compacted layers such as plow soles are present. The modeling approach adopted in this study helps to separate these effects and suggests that column height is a major driver of the observed differences, whereas compacted horizons may locally enhance solute retention. Therefore, too short soil columns may not accurately represent water and solute transport in field conditions. They could lead to overestimation of solute leaching potential and an underestimation of solute degradation, which could result in inaccurate risk assessments for contaminant migration to groundwater. Longer columns that capture the heterogeneity and preferential flow dynamics of natural soils should be used to improve the reliability of transport models and environmental risk assessments.

### 3.4 | Soil Core Sampling Method

Figure 4 shows the comparison of the $CaCl_2$ breakthrough curves for columns collected using a mechanical soil corer and by hand (leaching experiment no. 4).

The sampling method has a strong influence on the overall shape of the $CaCl_2$ breakthrough curves. They are strongly asymmetrically shifted to the left for columns made with the mechanical soil column auger, indicating strong preferential flows. Breakthrough curves for columns sampled by hand are more gradual, indicating fewer preferential flows and a greater portion of water and solute passing through the soil matrix. The solute is detected earlier in the leachates with a significantly shorter time ($p$ value = 0.045) to the first breakthrough ($T_{min}$) for the mechanical auger columns than for the hand columns where it is more retained. The peak occurred earlier ($p$ value = 0.048) for mechanical auger columns than for the hand columns, indicating greater solute retention in the columns made by hand. For columns sampled with the mechanical corer, the peak corresponds to the first water sample, indicating the presence of continuous preferential flow paths throughout the column that are not present in these hand-driven columns.

The sampling method also influences the height and width of the breakthrough curves. The maximum concentration of the peak ($C_{peak}$) is significantly higher ($p$ value = 0.023) for the mechanical auger columns. The majority of the solute is rapidly eluted from the columns sampled with the mechanical corer, with an average of 91.4% ± 7.4% of $CaCl_2$ recovered, compared to 63.3% ± 17.0% for the columns sampled by hand at the end of the experiment (Table 5). In addition, the total amount of pore volume eluted ($T_{tot}$) was significantly higher ($p$ value = 0.025) for the mechanical auger columns. The breakthrough curves of the mechanical auger columns show a $T_{peak}$ 4.9 times lower, a $C_{peak}$ (height) 2.0 times higher, and a $T_{tot}$ (width) 1.32 times higher than the columns sampled by hand. Visually, during the experiment, significant preferential flows were present between the soil column and the Plexiglas wall of the corer columns, generating a rapid flow of water. These continuous preferential flows are not present in the hand-driven columns. These flows are artificial and are created during core sampling. A possible cause would be the vibrations caused by the percussion hammer that is used to drive the column into the ground.

The average $R^2$ values obtained for the optimization of the water flow parameters are 0.99 ± 0.01 for the columns produced by a mechanical corer and 0.99 ± 0.01 for the columns taken by hand, indicating a suitable representation for both types of columns, despite very different water flows. For the two types of columns, the proportion of mobile zone is not significantly different. However, the $K_s$ is significantly higher ($p$ value = 0.003) for columns made with a mechanical corer than for columns taken by hand. Thus, at saturation, the water flows 1.5 times faster in the columns taken with the mechanical corer. The continuous preferential flows explain this high hydraulic conductivity and are mainly localized along the sides of the columns.

The solute transport parameters fitting resulted in a correct representation of solute transport with an average $R^2$ of 0.84 ± 0.12 for mechanical corer columns and 0.93 ± 0.06 for hand-sampled columns. The dispersivity, an indicator of the degree of preferential flows, is 25.3 times higher ($p$ value = 0.001) for the columns sampled with the corer compared to the columns driven by hand.

Interestingly, the $K_s$, the peak position, and the maximum relative concentration of the handmade columns are similar to the undisturbed columns of the leaching experiment no. 1. These similar results may be due to agricultural operations that homogenized the topsoil 1 month before these different columns were made.

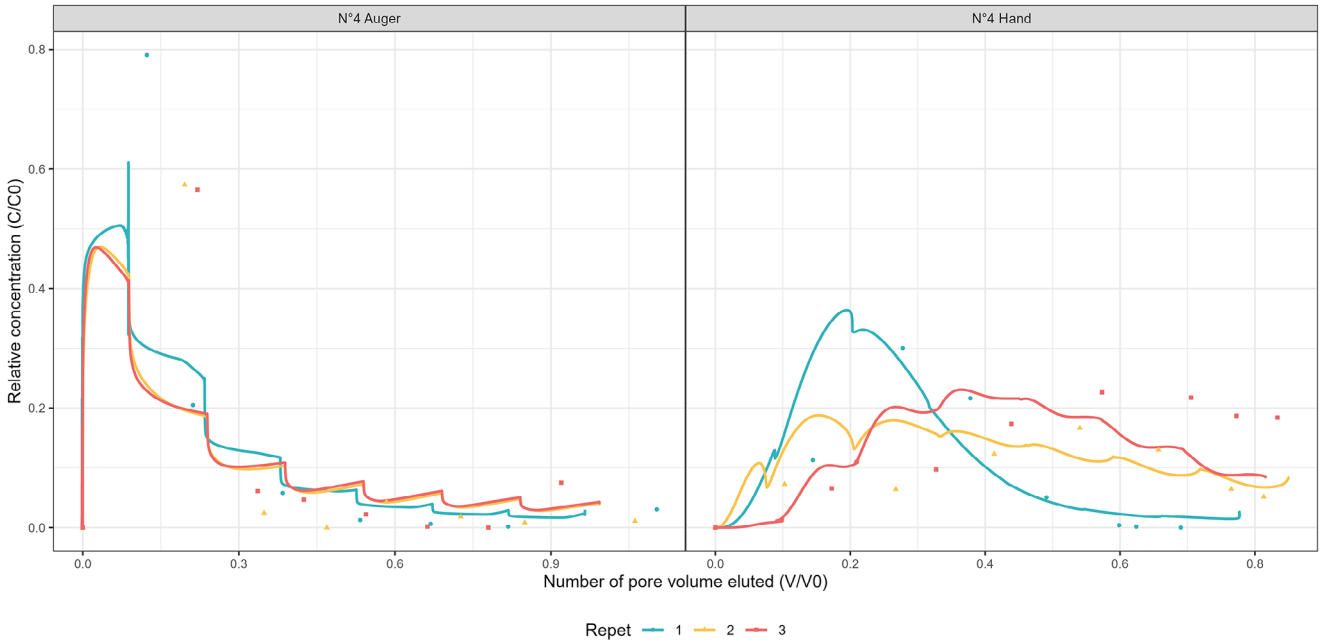


**FIGURE 4** | Measured and modeled breakthrough curves depicting the relative concentration ($C/C_0$) in the leachates plotted as a function of the number of pore volume eluted ($V/V_0$) for the $CaCl_2$ tracer for undisturbed columns (a) collected with the soil column cylinder auger and (b) collected by hand for the three replicates. The points correspond to the measured and the lines to the modeled data.

Therefore, although the mechanical corer in principle allows the sampling of undisturbed soil columns up to 1 m depth, this study suggests that these columns do not adequately represent water and solute fluxes. The vibrations of the hammer can create a gap between the soil column and the wall of the column. This gap generates continuous preferential flows and a rapid elution of the majority of the solute despite the wax poured at the soil–Plexiglas interface at the beginning of the experiment. As a result, hand-driven columns seem to be a better alternative to sample undisturbed soil columns and limit unnatural preferential flows.

## 4 | Conclusions and Perspectives

This study evaluated how common methodological choices in soil column experiments influence water flow, solute transport behavior, and the estimation of DP model parameters. By systematically varying soil structure, column diameter and length, and sampling method, the work provides a quantitative assessment of how experimental design affects the interpretation of leaching processes and associated contamination risks.

The results clearly demonstrate that soil structure is the dominant factor controlling solute transport dynamics. Intact soil columns exhibit strong physical nonequilibrium transport behavior driven by preferential flow through macropores, leading to earlier solute breakthrough, more asymmetric breakthrough curves, and greater dispersivity. In contrast, disturbed columns promote homogeneous flow conditions, resulting in delayed solute transport and reduced apparent heterogeneity. These differences imply that disturbed columns are poorly suited to represent solute transport under field conditions, as they tend to underestimate rapid contaminant migration and overestimate solute retention within the soil matrix.

Geometric characteristics of the columns also influence transport behavior, though to a lesser extent. Column diameter had limited impact on solute transport in disturbed soils, reflecting the homogeneity of the reconstructed matrix. Column height, however, significantly affected solute recovery and dispersivity in intact soils, highlighting the importance of capturing sufficient vertical heterogeneity and preferential pathways. Shorter columns may therefore overestimate solute leaching potential and underestimate solute degradation, leading to inaccurate risk assessments for groundwater contamination. Longer columns can therefore improve the reliability of transport models and environmental risk assessments.

The sampling method was shown to be a critical source of artifacts. Mechanical coring introduced artificial preferential flow along column walls, substantially altering transport parameters and breakthrough behavior. Hand-driven sampling, although more labor-intensive, provides a more reliable representation of natural soil structure and transport processes. These findings emphasize that sampling-induced disturbances can dominate solute transport responses and compromise model parameter estimation.

Despite the robustness of the experimental approach, several limitations should be acknowledged. Comparisons between disturbed and intact soil columns remain intrinsically challenging due to the natural heterogeneity of soil structure, even among replicates sampled at the same site. This complexity was further exacerbated by differences in sampling dates relative to agricultural operations, which influenced soil structure development and preferential flow pathways, thereby limiting strict comparability between experiments. From a risk assessment perspective, the results indicate that uncertainties in experimental design propagate directly into transport parameters used in numerical

models. However, the propagation of this parameter variability into solute leaching predictions was not explicitly assessed. Quantifying how uncertainties in parameters translate into uncertainty in groundwater contamination risk would require additional modeling scenarios.

Future research should therefore focus on quantifying how parameter uncertainty propagates into solute leaching predictions. Combining soil column experiments with field observations and sensitivity analyses would help identify which parameters most strongly control uncertainty in risk assessments. In addition, expanding the range of column configurations, soil types, and sampling conditions would allow the development of harmonization or correction approaches to improve the comparability of leaching studies. Ultimately, improving the representation of soil heterogeneity and preferential flow processes is essential for enhancing the reliability of contaminant transport models used in environmental management and regulatory decision-making.

This study allows researchers to better choose the experimental design according to the purpose of their experiments. By clarifying how these methodological factors influence leaching experiments and DP parameters, this work aims to support the development of standardized practices in soil column leaching research and improve the reliability of contamination risk assessments.

## Nomenclature

### Symbols

| | |
|---|---|
| $z$ | vertical coordinate, cm |
| $t$ | time, min |
| $h$ | water pressure head, cm |
| $\theta$ | total soil water content, $cm^3/cm^3$ |
| $\theta_{mo}$ | water content of mobile (macropore) region, $cm^3/cm^3$ |
| $\theta_{im}$ | water content of immobile (matrix) region, $cm^3/cm^3$ |
| $\theta_s$ | saturated soil water content, $cm^3/cm^3$ |
| $\theta_r$ | residual soil water content, $cm^3/cm^3$ |
| $\theta_{s,mo}$ | saturated water content of the mobile region, $cm^3/cm^3$ |
| $\theta_{s,im}$ | saturated water content of the immobile region, $cm^3/cm^3$ |
| $\theta_{r,mo}$ | residual water content of the mobile region, $cm^3/cm^3$ |
| $\theta_{r,im}$ | residual water content of the immobile region, $cm^3/cm^3$ |
| $K_s$ | saturated hydraulic conductivity, cm/min |
| $\alpha$ | van Genuchten shape parameter, 1/cm |
| $n$ | van Genuchten pore-size distribution parameter, – |
| $l$ | pore connectivity parameter, – |
| $h$ | water pressure head, cm |
| $a$ | angle between the flow direction and the vertical axis, – |
| $q_{mo}$ | volumetric water flux density in the mobile region, cm/min |
| $S_e$ | effective saturation, – |
| $S_e^{mo}$ | effective saturation of the mobile region, – |
| $S_e^{im}$ | effective saturation of the immobile region, – |
| $\Gamma_w$ | water mass transfer rate between regions, 1/min |
| $\omega$ | first-order water transfer coefficient between regions, 1/min |
| $c_{mo}$ | solute liquid concentration in mobile region, $g/cm^3$ |
| $c_{im}$ | solute liquid concentration in immobile region, $g/cm^3$ |
| $D_{mo}$ | dispersion coefficient in mobile region, $cm^2/min$ |
| $D_0$ | molecular diffusion coefficient in free water, $cm^2/min$ |
| $\lambda_{mo}$ | longitudinal dispersivity of the mobile region, cm |
| $v$ | pore water velocity, cm/min |
| $\Gamma_s$ | solute mass transfer rate between regions, $g/cm^3/min$ |
| $\omega_s$ | first-order solute mass transfer coefficient, 1/min |
| $\varphi(q,b)$ | objective function, – |
| $q_j^*(z,t_i)$ | observed variable at depth $z$ and time $t_i$, variable-dependent |
| $q_j(z,t_i,b)$ | simulated variable, variable-dependent |
| $b$ | vector of optimized parameters, – |
| $m$ | number of measurement sets, – |
| $n$ | number of observations per set, – |
| $v_j$ | weighting factor for measurement set $j$, – |
| $w_{ij}$ | weighting factor for observation $i$, – |
| $C/C_0$ | relative solute concentration, – |
| $V/V_0$ | relative pore volume, – |
| $T_{min}$ | relative pore volume at tracer arrival, – |
| $C_{peak}$ | maximum relative concentration, – |
| $T_{peak}$ | relative pore volume at peak concentration, – |
| $R^2$ | coefficient of determination, – |
| SSQ | sum of squares, – |

## Conflicts of Interest

The authors declare no conflicts of interest.

## Data Availability Statement

The data that support the findings of this study are available on request from the corresponding author. The data are not publicly available due to privacy or ethical restrictions.

## References

1. N. Baran, N. Surdyk, and C. Auterives, "Pesticides in Groundwater at a National Scale (France): Impact of Regulations, Molecular Properties, Uses, Hydrogeology and Climatic Conditions," *Science of the Total Environment* 791 (2021): 148137, https://doi.org/10.1016/j.scitotenv.2021.148137.

2. EurEau. *Europe's Water in Figures an Overview of the European Drinking Water and Waste Water Sectors* (Brussels, 2021).

3. K. Kiefer, A. Müller, H. Singer, and J. Hollender, "New Relevant Pesticide Transformation Products in Groundwater Detected Using Target and Suspect Screening for Agricultural and Urban Micropollutants With

LC-HRMS," *Water Research* 165 (2019): 114972, https://doi.org/10.1016/j.watres.2019.114972.

4. D. Pietrzak, J. Kania, G. Malina, E. Kmiecik, and K. Wator, "Pesticides From the EU First and Second Watch Lists in the Water Environment," *Clean—Soil, Air, Water* 47 (2019): 1800376, https://doi.org/10.1002/clen.201800376.

5. V. Barba, J. M. Marín-Benito, M. J. Sánchez-Martín, and M. S. Rodríguez-Cruz, "Transport of 14C-Prosulfocarb Through Soil Columns Under Different Amendment, Herbicide Incubation and Irrigation Regimes," *Science of the Total Environment* 701 (2020): 134542, https://doi.org/10.1016/j.scitotenv.2019.134542.

6. S. Cueff, L. Alletto, M. Bourdat-Deschamps, P. Benoit, and V. Pot, "Water and Pesticide Transfers in Undisturbed Soil Columns Sampled From a Stagnic Luvisol and a Vermic Umbrisol Both Cultivated Under Conventional and Conservation Agriculture," *Geoderma* 377 (2020): 114590, https://doi.org/10.1016/j.geoderma.2020.114590.

7. A. Imig, L. Augustin, J. Groh, et al., "Fate of Herbicides in Cropped Lysimeters: 2. Leaching of Four Maize Herbicides Considering Different Processes," *Vadose Zone Journal* 22 (2023): 1–14, https://doi.org/10.1002/vzj2.20275.

8. M. Siedt, A. Schäffer, K. E. C. Smith, M. Nabel, M. Roß-Nickoll, and J. T. van Dongen, "Comparing Straw, Compost, and Biochar Regarding Their Suitability as Agricultural Soil Amendments to Affect Soil Structure, Nutrient Leaching, Microbial Communities, and the Fate of Pesticides," *Science of the Total Environment* 751 (2021): 141607, https://doi.org/10.1016/j.scitotenv.2020.141607.

9. A. E. Akay Demir, F. B. Dilek, and U. Yetis, "A New Screening Index for Pesticides Leachability to Groundwater," *Journal of Environmental Management* 231 (2019): 1193–1202, https://doi.org/10.1016/j.jenvman.2018.11.007.

10. European Commission. Assessing Potential for Movement of Active Substances and Their Metabolites to Ground Water in the EU Report of the FOCUS Ground Water Work Group (European Commission, 2014).

11. H. Labite, F. Butler, and E. Cummins, "A Review and Evaluation of Plant Protection Product Ranking Tools Used in Agriculture," *Human & Ecological Risk Assessment* 17 (2011): 300–327, https://doi.org/10.1080/10807039.2011.552392.

12. M. Arias-Estévez, E. López-Periago, E. Martínez-Carballo, J. Simal-Gándara, J. C. Mejuto, and L. García-Río, "The Mobility and Degradation of Pesticides in Soils and the Pollution of Groundwater Resources," *Agriculture Ecosystems and Environment* 123 (2008): 247–260, https://doi.org/10.1016/j.agee.2007.07.011.

13. M. A. Malla, S. Gupta, A. Dubey, A. Kumar, and S. Yadav, "Contamination of Groundwater Resources by Pesticides," in *Contamination of Water: Health Risk Assessment and Treatment Strategies* (Academic Press, 2021), https://doi.org/10.1016/B978-0-12-824058-8.00023-2.

14. J. Dusek, M. Dohnal, M. Snehota, M. Sobotkova, C. Ray, and T. Vogel, "Transport of Bromide and Pesticides Through an Undisturbed Soil Column: A Modeling Study With Global Optimization Analysis," *Journal of Contaminant Hydrology* 175–176 (2015): 1–16, https://doi.org/10.1016/j.jconhyd.2015.02.002.

15. G. M. Kahl, Y. Sidorenko, and B. Gottesbüren, "Local and Global Inverse Modelling Strategies to Estimate Parameters for Pesticide Leaching From Lysimeter Studies," *Pest Management Science* 71 (2015): 616–631, https://doi.org/10.1002/ps.3914.

16. R. Sur, C. Kley, and S. Sittig, "Field Leaching Study—Inverse Estimation of Degradation and Sorption Parameters for a Mobile Soil Metabolite and Its Pesticide Parent," *Environmental Pollution* 310 (2022): 119794, https://doi.org/10.1016/j.envpol.2022.119794.

17. J. M. Köhne, S. Köhne, and J. Šimůnek, "A Review of Model Applications for Structured Soils: B) Pesticide Transport," *Journal of Contaminant Hydrology* 104 (2009): 36–60, https://doi.org/10.1016/j.jconhyd.2008.10.003.

18. I. Varvaris, Z. Pittaki-Chrysodonta, C. Duus Børgesen, and B. V. Iversen, "Parameterization of Two-Dimensional Approaches in HYDRUS-2D: Part 1. Simulating Water Flow Dynamics at the Field Scale," *Soil Science Society of America Journal* 85 (2021): 1578–1599, https://doi.org/10.1002/saj2.20307.

19. J. M. Köhne, S. Köhne, and J. Šimůnek, "Multi-Process Herbicide Transport in Structured Soil Columns: Experiments and Model Analysis," *Journal of Contaminant Hydrology* 85 (2006): 1–32, https://doi.org/10.1016/j.jconhyd.2006.01.001.

20. V. Pot, J. Šimůnek, P. Benoit, Y. Coquet, A. Yra, and M. J. Martínez-Cordón, "Impact of Rainfall Intensity on the Transport of Two Herbicides in Undisturbed Grassed Filter Strip Soil Cores," *Journal of Contaminant Hydrology* 81 (2005): 63–88, https://doi.org/10.1016/j.jconhyd.2005.06.013.

21. J. Dusek, M. Dohnal, T. Vogel, and C. Ray, "Field Leaching of Pesticides at Five Test Sites in Hawaii: Modeling Flow and Transport," *Pest Management Science* 67 (2011): 1571–1582, https://doi.org/10.1002/ps.2217.

22. T. Katagi, "Soil Column Leaching of Pesticides," *Reviews of Environment Contamination and Toxicology* 221 (2013): 1–105, https://doi.org/10.1007/978-1-4614-4448-0_1..

23. M. Aliste, G. Pérez-Lucas, I. Garrido, J. Fenoll, and S. Navarro, "Mobility of Insecticide Residues and Main Intermediates in a Clay-Loam Soil, and Impact of Leachate Components on Their Photocatalytic Degradation," *Chemosphere* 274 (2021): 129965, https://doi.org/10.1016/j.chemosphere.2021.129965.

24. M. A. Khan and C. D. Brown, "Influence of Commercial Formulation on Leaching of Four Pesticides Through Soil," *Science of the Total Environment* 573 (2016): 1573–1579, https://doi.org/10.1016/j.scitotenv.2016.09.076.

25. P. Ortega, E. Sánchez, E. Gil, and V. Matamoros, "Use of Cover Crops in Vineyards to Prevent Groundwater Pollution by Copper and Organic Fungicides. Soil Column Studies," *Chemosphere* 303 (2022): 134975, https://doi.org/10.1016/j.chemosphere.2022.134975.

26. V. Pot, P. Benoit, M. L. Menn, O. M. Eklo, T. Sveistrup, and J. Kværner, "Metribuzin Transport in Undisturbed Soil Cores Under Controlled Water Potential Conditions: Experiments and Modelling to Evaluate the Risk of Leaching in a Sandy Loam Soil Profile," *Pest Management Science* 67 (2010): 397–407, https://doi.org/10.1002/ps.2077.

27. J. K. Koestel, T. Norgaard, N. M. Luong, et al., "Links Between Soil Properties and Steady-State Solute Transport Through Cultivated Topsoil at the Field Scale," *Water Resources Research* 49 (2013): 790–807, https://doi.org/10.1002/wrcr.20079.

28. A. M. Sadeghi, A. R. Isensee, and A. Shirmohammadi, "Influence of Soil Texture and Tillage on Herbicide Transport," *Chemosphere* 41 (2000): 1327–1332, https://doi.org/10.1016/S0045-6535(00)00028-X.

29. C. N. Albers, U. E. Bollmann, N. Badawi, and A. R. Johnsen, "Leaching of 1,2,4-Triazole From Commercial Barley Seeds Coated With Tebuconazole and Prothioconazole," *Chemosphere* 286 (2022): 131819, https://doi.org/10.1016/j.chemosphere.2021.131819.

30. A. Imig, L. Augustin, J. Groh, et al., "Fate of Herbicides in Cropped Lysimeters: 1. Influence of Different Processes and Model Structure on Vadose Zone Flow," *Vadose Zone Journal* 22 (2023b): 1–13, https://doi.org/10.1002/vzj2.20265.

31. J. K. Koestel, J. Moeys, and N. J. Jarvis, "Meta-Analysis of the Effects of Soil Properties, Site Factors and Experimental Conditions on Solute Transport," *Hydrology and Earth System Sciences* 16 (2012): 1647–1665, https://doi.org/10.5194/hess-16-1647-2012.

32. M. Bromly, C. Hinz, and L. A. G. Aylmore, "Relation of Dispersivity to Properties of Homogeneous Saturated Repacked Soil Columns," *European Journal of Soil Science* 58 (2007): 293–301, https://doi.org/10.1111/j.1365-2389.2006.00839.x.

33. A. Vincent, P. Benoit, V. Pot, I. Madrigal, L. Delgado-Moreno, and C. Labat, "Impact of Different Land Uses on the Migration of Two Herbicides in a Silt Loam Soil: Unsaturated Soil Column Displacement Studies,"

*European Journal of Soil Science* 58 (2007): 320–328, https://doi.org/10.1111/j.1365-2389.2006.00844.x.

34. L. Bégin, J. Fortin, and J. Caron, "Evaluation of the Fluoride Retardation Factor in Unsaturated and Undisturbed Soil Columns," *Soil Science Society of America Journal* 67 (2003): 1635–1646, https://doi.org/10.2136/sssaj2003.1635.

35. J. Lewis and J. Sjöstrom, "Optimizing the Experimental Design of Soil Columns in Saturated and Unsaturated Transport Experiments," *Journal of Contaminant Hydrology* 115 (2010): 1–13, https://doi.org/10.1016/j.jconhyd.2010.04.001.

36. FAO. *World Reference Base for Soil Resources 2014—International Soil Classification System for Naming Soils and Creating Legends for Soil Maps* World Soil Resources Reports (FAO, 2015), https://doi.org/10.1038/nnano.2009.216.

37. M. A. Plummer, L. C. Hull, and D. T. Fox, "Transport of Carbon-14 in a Large Unsaturated Soil Column," *Vadose Zone Journal* 3 (2004): 109–121, https://doi.org/10.2136/vzj2004.1090.

38. E. L. Arthur, P. J. Rice, P. J. Rice, T. A. Anderson, and J. R. Coats, "Mobility and Degradation of Pesticides and Their Degradates in Intact Soil Columns," in *The Lysimeter Concept, Environmental Behavior of Pesticides*, ed. F. Führ, R. Hance, J. Plimmer, and J. Nelson (American Chemical Society, 1998), 88–114, https://doi.org/10.1021/bk-1998-0699.ch007.

39. A. R. Isensee and A. M. Sadeghi, "Laboratory Apparatus for Studying Pesticide Leaching in Intact Soil Cores," *Chemosphere* 25 (1992): 581–590, https://doi.org/10.1016/0045-6535(92)90289-4.

40. C. Pirlot, A.-C. Renard, C. De Clerck, and A. Degré, "How Does Soil Water Retention Change Over Time? A Three-Year Field Study Under Several Production Systems," *European Journal of Soil Science* 75 (2024): 13558, https://doi.org/10.1111/ejss.13558.

41. N. Glæsner, E. Diamantopoulos, J. Magid, C. Kjaergaard, and H. H. Gerke, "Modeling Solute Mass Exchange Between Pore Regions in Slurry-Injected Soil Columns During Intermittent Irrigation," *Vadose Zone Journal* 17 (2018): 180006, https://doi.org/10.2136/vzj2018.01.0006.

42. J. Šimůnek, M. T. Genuchten, and M. Šejna, "Development and Applications of the HYDRUS and STANMOD Software Packages and Related Codes," *Vadose Zone Journal* 7 (2008): 587–600, https://doi.org/10.2136/vzj2007.0077.

43. D. W. Marquardt, "An Algorithm for Least-Squares Estimation of Nonlinear Parameters," *Journal of the Society for Industrial and Applied Mathematics* 11 (1963): 431–441, https://doi.org/10.1137/0111030.

44. J. Šimůnek, M. T. van Genuchten, M. M. Gribb, and J. W. Hopmans, "Parameter Estimation of Unsaturated Soil Hydraulic Properties From Transient Flow Processes," *Soil and Tillage Research* 47 (1998): 27–36, https://doi.org/10.1016/S0167-1987(98)00069-5.

45. J. Šimunek, M. T. Van Genuchten, and Jacques, "Solute Transport During Variably Saturated Flow—Inverse Methods," in *Methods of Soil Analysis. Part 4. Physical Methods*, ed. J. H. Dane and G. C. Topp (Soil Science Society of America, Inc., 2002), 1435–1449.

46. J. Šimůnek, N. J. Jarvis, M. T. Van Genuchten, and A. Gärdenäs, "Review and Comparison of Models for Describing Non-Equilibrium and Preferential Flow and Transport in the Vadose Zone," *Journal of Hydrology* 272 (2003): 14–35, https://doi.org/10.1016/S0022-1694(02)00252-4.

47. M. T. van Genuchten and P. J. Wierenga, "Mass Transfer Studies in Sorbiong Porous Media," *Soil Science Society of America Journal* 40 (1976): 473–480.

48. M. T. van Genuchten, "A Closed-Form Equation for Predicting the Hydraulic Conductivity of Unsaturated Soils," *Soil Science Society of America Journal* 44 (1980): 892–898, https://doi.org/10.2136/sssaj1980.03615995004400050002x.

49. Y. Mualem, "A New Model for Predicting the Hydraulic Conductivity of Unsaturated Porous Media," *Water Resources Research* 12 (1976): 513–522, https://doi.org/10.1029/WR012i003p00513.

50. S. L. Graham, M. S. Srinivasan, N. Faulkner, and S. Carrick, "Soil Hydraulic Modeling Outcomes With Four Parameterization Methods : Comparing Soil Description and Inverse Estimation Approaches," *Vado* 17 (2018): 170002, https://doi.org/10.2136/vzj2017.01.0002.

51. M. G. Schaap, F. J. Leij, and M. T. Van Genuchten, "ROSETTA : A Computer Program for Estimating Soil Hydraulic Parameters With Hierarchical Pedotransfer Functions," *Journal of Hydrology* 251 (2001): 163–176, https://doi.org/10.1016/S0022-1694(01)00466-8.

52. H. H. Gerke and M. T. van Genuchten, "Evaluation of a First-Order Water Transfer Term for Variably Saturated Dual-Porosity Flow Models," *Water Resources Research* 29 (1993): 1225–1238, https://doi.org/10.1029/92WR02467.

53. J. Simunek, O. Wendroth, N. Wypler, and M. T. van Genuchten, "Non-Equilibrium Water Flow Characterized by Means of Upward Infiltration Experiments," *European Journal of Soil Science* 52 (2001): 13–24, https://doi.org/10.1046/j.1365-2389.2001.00361.x.

54. R. Kodešová, J. Kozák, J. Šimůnek, and O. Vacek, "Single and Dual-Permeability Models of Chlorotoluron Transport in the Soil Profile," *Plant, Soil and Environment* 51 (2005): 310–315, https://doi.org/10.17221/3591-pse.

55. J. Šimůnek, M. Šejna, H. Saito, M. Sakai, and M. T. Van Genuchten, *The HYDRUS-1D Software Package for Simulating the One-Dimensional Movement of Water, Heat, and Multiple Solutes in Variably-Saturated Media*, Version 4.08. Hydrus Software Series (Department of environmental sciences, University of California Riverside, 2009).

56. J. M. Köhne, S. Köhne, B. P. Mohanty, and J. Šimůnek, "Inverse Mobile-Immobile Modeling of Transport During Transient Flow: Effects of Between-Domain Transfer and Initial Water Content," *Vadose Zone Journal* 3 (2004): 1309–1321, https://doi.org/10.2136/vzj2004.1309.

57. J. Mertens, R. Stenger, and G. F. Barkle, "Multiobjective Inverse Modeling for Soil Parameter Estimation and Model Verification," *Vadose Zone Journal* 5 (2006): 917–933, https://doi.org/10.2136/vzj2005.0117.

58. J. Šimůnek and M. T. Genuchten, "Modeling Nonequilibrium Flow and Transport Processes Using HYDRUS," *Vadose Zone Journal* 7 (2008): 782–797, https://doi.org/10.2136/vzj2007.0074.

59. J. Vanderborght and H. Vereecken, "Review of Dispersivities for Transport Modeling in Soils," *Vadose Zone Journal* 6 (2007): 29–52, https://doi.org/10.2136/vzj2006.0096.

60. M. Flury and T. F. Gimmi, "Solute Diffusion," in *Methods of Soil Analysis*, ed. H. Jacob and G. Clarke (Soil Science Society of America, 2002), 1323–1351, https://doi.org/10.2136/sssabookser5.4.c55.

61. F. Abbasi, D. Jacques, J. Simunek, J. Feyen, and M. T. van Genuchten, "Inverse Estimation of Soil Hydraulic and Solute Transport Parameters From Transient Field Experiments: Heterogeneous Soil," *American Society of Agricultural Engineers* 46 (2003): 1097–1111, https://doi.org/10.13031/2013.13961.

62. S. K. Kamra, B. Lennartz, M. T. Van Genuchten, and P. Widmoser, "Evaluating Non-Equilibrium Solute Transport in Small Soil Columns," *Journal of Contaminant Hydrology* 48 (2001): 189–212, https://doi.org/10.1016/S0169-7722(00)00156-X.

63. N. Singh, H. Kloeppel, and W. Klein, "Movement of Metolachlor and Terbuthylazine in Core and Packed Soil Columns," *Chemosphere* 47 (2002): 409–415, https://doi.org/10.1016/S0045-6535(01)00322-8.

64. J. L. Celestino Ladu and D. R. Zhang, "Modeling Atrazine Transport in Soil Columns With HYDRUS-1D," *Water Science and Engineering* 4 (2011): 258–269, https://doi.org/10.3882/j.issn.1674-2370.2011.03.003.

65. L. Cox, M. J. Calderón, M. C. Hermosín, and J. Cornejo, "Leaching of Clopyralid and Metamitron Under Conventional and Reduced Tillage Systems," *Journal of Environmental Quality* 28 (1999): 605–610, https://doi.org/10.2134/jeq1999.00472425002800020026x.

66. S. Morsali, H. Babazadeh, S. Shahmohammadi-Kalalagh, and H. Sedghi, "Simulating Zn, Cd and Ni Transport in Disturbed and Undisturbed Soil Columns: Comparison of Alternative Models," *International Journal of Environmental Research* 13 (2019): 721–734, https://doi.org/10.1007/s41742-019-00212-w.

67. W. Van Beinum, S. Beulke, C. Fryer, and C. Brown, "Lysimeter Experiment to Investigate the Potential Influence of Diffusion-Limited Sorption on Pesticide Availability for Leaching," *Journal of Agricultural and Food Chemistry* 54 (2006): 9152–9159, https://doi.org/10.1021/jf061850m..

68. C. Porfiri, J. C. Montoya, W. C. Koskinen, and M. P. Azcarate, "Adsorption and Transport of Imazapyr Through Intact Soil Columns Taken From Two Soils Under Two Tillage Systems," *Geoderma* 251–252 (2015): 1–9, https://doi.org/10.1016/j.geoderma.2015.03.016.

## Supporting Information

Additional supporting information can be found online in the Supporting Information section.

**Supporting File 1**: clen70140-sup-0001-SuppMat.docx.

**Supporting File 2**: clen70140-sup-0002-Tables.xlsx.